

Article

Optimizing Chitin Extraction and Chitosan Production from House Cricket Flour

Andrea Espinosa-Solís ¹, Angélica Velázquez-Segura ¹, Carlos Lara-Rodríguez ¹, Luz María Martínez ¹ , Cristina Chuck-Hernández ^{2,*}  and Lucio Rodríguez-Sifuentes ^{3,*} 

¹ School of Engineering and Sciences, Tecnológico de Monterrey, Eugenio Garza Sada 2501, Col. Tecnológico, Monterrey 64849, Mexico; a00825433@exatec.tec.mx (A.E.-S.); a00825810@exatec.tec.mx (A.V.-S.); a01283067@exatec.tec.mx (C.L.-R.); luzvidea@tec.mx (L.M.M.)

² Institute for Obesity Research, Tecnológico de Monterrey, Eugenio Garza Sada 2501, Col. Tecnológico, Monterrey 64849, Mexico

³ Facultad de Ciencias Biológicas, Universidad Autónoma de Coahuila, Carretera Torreón-Matamoros Km 7.5, Torreón 27104, Mexico

* Correspondence: cristina.chuck@tec.mx (C.C.-H.); lucio.rodriguez@uadec.edu.mx (L.R.-S.)

Abstract: Chitin and its derivative, chitosan, have diverse applications in fields such as agriculture, medicine, and biosensors, amongst others. Extraction is primarily conducted from marine sources, such as crustaceans, which have been the focus of process optimization studies. However, there are other sources that are more readily available, such as insects, where insufficient research has been conducted. The house cricket (*Acheta domesticus*) is a promising source for chitin extraction because of its high chitin content, availability, and short lifespan. Modern chemical chitin extraction methods have not been standardized due to the use of different reagents, molar concentrations, temperatures, and reaction times across publications. Therefore, in this study, the composition of *Acheta domesticus* cricket flour was determined: 2.62% humidity, 4.3% ash content, 56.29% protein, 13.35% fat, 23.44% carbohydrates, and 15.71% crude fiber content. After a drying, defatting, demineralization, deproteinization, and bleaching process, chitin extraction was performed, and chitosan was obtained via a deacetylation reaction. The demineralization process was standardized at 30 °C for 3 h using HCl 2 M, resulting in 95.85 ± 0.012%. The deproteinization process was optimized at 80 °C for 45 min using NaOH 2.56 M, yielding 43.23 ± 1.25%. Finally, the identity and physico-chemical characteristics of the compounds were confirmed and determined through characterization with Fourier-Transform Infrared Spectroscopy, X-ray Diffraction, Scanning Electron Microscopy, and Differential Scanning Calorimetry.

Keywords: *Acheta domesticus*; bleaching; deacetylation; demineralization; deproteinization; insects



Citation: Espinosa-Solís, A.; Velázquez-Segura, A.; Lara-Rodríguez, C.; Martínez, L.M.; Chuck-Hernández, C.; Rodríguez-Sifuentes, L. Optimizing Chitin Extraction and Chitosan Production from House Cricket Flour. *Processes* **2024**, *12*, 464. <https://doi.org/10.3390/pr12030464>

Academic Editors: Xingyuan Huang, Mengshan Li and Shiyu Jiang

Received: 9 January 2024

Revised: 10 February 2024

Accepted: 16 February 2024

Published: 25 February 2024



Copyright: © 2024 by the authors. Licensee MDPI, Basel, Switzerland. This article is an open access article distributed under the terms and conditions of the Creative Commons Attribution (CC BY) license (<https://creativecommons.org/licenses/by/4.0/>).

1. Introduction

Chitin is the second most abundant polymer in nature after cellulose. This biopolymer, along with its derived compound chitosan, has diverse applications in the agriculture, medicine, water treatment, cosmetics, textile, and biosensor industries, among others [1]. Due to the versatile nature of both compounds, chitin extraction and chitosan production are highly valuable processes that are generally carried out using sources such as insects, crustaceans, and fish [1,2].

The extraction of chitin is typically carried out from biological residues in the fishing industry, specifically from crustacean exoskeletons. However, these can only be obtained in sufficient quantities during seasons throughout the year, leading to limited availability and volume. Therefore, the search for an alternative source of chitin is highly relevant. Insects have been found to possess similar chitin contents to those of crustaceans, with the advantage of shorter reproductive cycles, making them an attractive new source for chitin extraction. Specifically, the cricket species *Acheta domesticus* has shown great promise as an

alternative chitin source, as it is readily available and can be acquired in large quantities, since it is considered a pest in the agriculture industry [3].

To obtain purified chitin from crustacean, insect, or fish flour, a two-step process involving demineralization (DM) and deproteinization (DP) is required. In the DM step, acid hydrolysis is employed to digest the mineral content of the sample, while in the DP step; the sample undergoes alkaline treatment to eliminate its proteins. Subsequently, the obtained chitin undergoes a whitening process for purification and is then transformed into chitosan through a deacetylation (DA) reaction, changing the acetamide groups into amines [3,4].

It has been shown that a wide variety of chitin extraction techniques depend on the characteristics of the source [5]. Studies carried out on chitin extraction and chitosan generation from insects reveal significant variations in reaction conditions, particularly in the concentration of reactants for both processes (ranging from 0.5 M to 1 M for DM and from 1 M to 4 M for DP). However, there is consistency in the use of sodium hydroxide and hydrochloric acid for DP and DM, respectively. The reaction time and temperature also exhibit variations, with durations ranging from 30 min to 2 h for DM and 2 to 24 h for DP, and temperatures spanning from 25 °C to 97 °C for DM and 82 °C to 175 °C for DP. These diverse reaction conditions result in chitin extraction yields ranging from 4.3% to 20% and 2.4% to 24% for chitosan obtention [6–9].

Most of the literature addressing the optimization and standardization of the chitin extraction process has focused on crustacean sources. However, there is currently no optimized and standardized chitin extraction process for insect sources, particularly for the cricket *Acheta domesticus* [10]. Typically, the optimization processes involve the use of statistical methods such as composite core designs, Box-Behnken response surface design, and the Taguchi method. Alternatively, new technologies like artificial neural networks (ANN) have been employed [11–13]. These optimization efforts have been carried out in various studies with crustacean sources. The main distinctions among them lie in the different reaction conditions, times, and temperatures applied to DM and DP stages of the chitin extraction process. These factors are highly specific to each crustacean species under study, and the optimization process itself depends on the statistical method employed [14–19].

Since there are currently no optimized or standardized protocols published previously for chitin extraction from insect sources, and having identified the most relevant stages of the extraction process (DM and DP), the objective of this study was to establish an optimized chitin extraction protocol for insects, specifically focusing on the cricket *Acheta domesticus*. Furthermore, the polymers obtained were characterized by X-ray Diffraction (XRD), Fourier-Transform Infrared Spectroscopy (FTIR), Differential Scanning Calorimetry (DSC), and Scanning Electron Microscopy (SEM). This study contributes to establishing the concentration, time, and temperature conditions used in the DM and DP processes for obtaining chitin from the house cricket. This will enable the development of a standardized and specific methodology for chitin extraction from insects, instead of employing methodologies designed for crustaceans.

2. Methodology

2.1. Compositional Analysis of Cricket Flour

Cricket flour from the species *Acheta domesticus* was acquired from the Mexican company “Bicho”, Ensenada, Mexico. A compositional analysis of this flour was performed (humidity, ashes, fat, protein, and crude fiber determination) according to protocols provided by the Center for Research and Protein Development (CIDPRO) from Tecnológico de Monterrey, Mexico, which are based on AOAC protocols [20–26].

2.1.1. Humidity Determination

As the initial step in the compositional analysis, it is crucial to determine the humidity levels in the flour sample for the subsequent calculations to be reported on a dry basis. To

achieve this, six samples were weighed and placed in aluminum capsules. Subsequently, they were subjected to heating in a VWR stove (Radnor, PA, USA) at 100 °C for 24 h. Finally, the samples were re-weighed, and the humidity percentage was calculated using Equation (1) [20]:

$$\% \text{ Humidity} = \frac{\text{Weight of humid sample} - \text{Weight of dry sample}}{\text{Weight of humid sample}} \times 100\% \quad (1)$$

2.1.2. Ash Content Determination

Three samples were weighed in previously weighed porcelain crucibles and then placed in a Fisher Scientific Carbolite™ CWF Chamber Furnace (Sheffield, Yorks, UK) at 900 °C for 4 h. Subsequently, the cooled crucibles were weighed, and the ash content was determined using Equation (2) [21,25]:

$$\% \text{ Ash (dry weight)} = \frac{\text{Ash weight}}{\text{Weight of dry sample}} \times 100\% \quad (2)$$

2.1.3. Fat Content Determination

The fat content determination was carried out using the Goldfish method. Five samples were weighed and placed in glass containers with 30 mL of pure petroleum ether (Desarrollo de Especialidades Químicas) in the Labconco Goldfish equipment (Kansas City, MO, USA) in order to perform fat extraction for 4 h. Once the solvent was almost completely evaporated, the containers were removed from the Goldfish extractor and placed in an oven at 100 °C overnight. Subsequently they were allowed to cool and were weighed to determine the fat content in the sample using Equation (3) [22]:

$$\% \text{ Fat content (dry weight)} = \frac{\text{Weight of glass with fat}}{\text{Weight of dry sample}} \times 100\% \quad (3)$$

2.1.4. Protein Content Determination

The protein content was determined using the Micro Kjeldahl method, which relies on assessing the total nitrogen content. All reagents were purchased from Desarrollo de Especialidades Químicas. Six samples, each weighing 0.1 g, of dry cricket flour were measured alongside 2.04 to 2.05 g of digestion salts (for 100 g: 97.8 g 99% anhydrous potassium sulphate and 2.2 g 98% copper sulphate pentahydrate). This mixture was placed in Micro Kjeldahl flasks and allowed to react with 3.5 mL of concentrated (95 to 99%) sulphuric acid for 4 h in pre-heated digesters. After the reaction, and when no more dark spots were visible in the flasks, the samples underwent distillation for 5 min using 50% sodium hydroxide solution and a Labconco Rapid Still I distiller (Kansas City, MO, USA). Subsequently, titration was performed using 0.2 N hydrochloric acid [23,24]. Finally, the percentage of protein content was determined using Equations (4) and (5), incorporating a nitrogen conversion factor of 5.25:

$$\% \text{ N}_2 = \frac{\text{Used mL HCl} * \text{HCl normality} * 0.014}{\text{Weight of dry sample}} \times 100\% \quad (4)$$

$$\% \text{ Protein (dry weight)} = \frac{\% \text{ N}_2 * \text{conversion factor}}{100 - \% \text{ Humidity}} \times 100\% \quad (5)$$

2.1.5. Crude Fiber Content Determination

All reagents were purchased from Desarrollo de Especialidades Químicas. Six samples underwent acid hydrolysis with 200 mL of 1.25% sulfuric acid per 1.5 g of previously degreased flour at boiling point for 30 min. Subsequently, the samples were filtered using dry filter papers and immersed in 200 mL of 1.25% sodium hydroxide at boiling point for an additional 30 min. Following this step, the samples were filtered again and rinsed with

hot distilled water and 20 mL of 96% ethanol. Next, the samples were placed on new dry ashless filter paper and placed in an oven at 60 °C for 12 h. Afterward, they were weighed, and the crude fiber percentage was calculated by subjecting them to a furnace at 550 °C for 6 h. The ashes were weighed, and Equation (6) was used in the calculation [25,26].

$$\% \text{ Crude fiber (dry weight)} = \frac{\text{Crucible weight with dry residue(g)} - \text{Crucible weight with ashes(g)}}{\text{Sample weight(g)}} \times 100\% \quad (6)$$

2.2. Sample Preparation

The cricket flour was treated before chitin extraction by degreasing it to eliminate interferences. This involved placing 100 g of flour with 400 mL of 98.5% hexane (J.T. Baker) in a VWR Rf1575 incubator (Radnor, PA, USA) at 45 °C and 125 rpm for 4 h. This process was repeated twice. Subsequently, the sample was transferred to an aluminum tray and allowed to dry completely. To confirm the successful degreasing of the cricket flour, three samples of 2 g each were taken and analyzed using the Goldfish method to calculate the percentage of fat content using Equation (3). The degreased cricket flour obtained was then used in the subsequent steps.

2.3. Chitin Extraction from Cricket Flour

The optimization and standardization process of the chitin extraction protocol was carried out in two stages: DM and DP. The purpose of each stage was to remove minerals from the degreased sample and eliminate proteins in the cricket flour, respectively. The methodology described is based on the one used by Ibitoye et al. [27].

2.3.1. Demineralization (DM)

A factorial design comprising 3 factors with 2 levels was established: temperature (30 °C and 65 °C), time (3 h and 6 h), and molar concentration of HCl (1 M and 2 M) (J.T. Baker). Table 2 displays the 8 experimental conditions along with their respective results, which can be seen in the Results section.

Each experiment was performed in triplicate with 5 g samples and 50 mL of HCl. The acid concentration, temperature, and time were established according to the experimental design outlined in Table 2. Samples were filtered and rinsed with hot distilled water until they reached a pH between 6 and 7. Subsequently, they were placed in an oven at 60 °C and calcinated in a furnace at 900 °C to calculate the percentage of demineralization (%DM) (Equation (7)).

$$\% \text{DM} = \frac{\text{Mineral content before treatment} - \text{Mineral content after treatment}}{\text{Mineral content before treatment}} \times 100\% \quad (7)$$

Once the battery of experiments was completed, Minitab Version 19.2020.1.0 (State College, PA, USA) was used to analyze the data. An analysis of variance (ANOVA) at a confidence level of 95% ($p < 0.05$) was conducted to identify the factors that had the most significant impact on the demineralization process. Additionally, a Tukey test with a 95% confidence interval was performed to assess statistical differences among experimental conditions. This was carried out to select the condition that maximizes the %DM with the least energy expenditure.

The degreased cricket flour was demineralized under the selected conditions. To ensure proper demineralization, three samples were taken, and the %DM was calculated using Equation (7). The subsequent steps involved the use of this demineralized flour.

2.3.2. Deproteinization (DP)

To optimize the DP process, a Box–Behnken surface response design with three factors and three levels was conducted: temperature (60 to 80 °C), time (15 to 45 min), and NaOH concentration (1 to 3 M) (Desarrollo de Especialidades Químicas). The fifteen generated experiments are presented in Table 4.

It has been reported that the reaction time for the DP process takes hours [27]. However, due to the extreme conditions at each level for every factor, it was decided to scale down the time to minutes to preserve the integrity of the samples and to avoid wasting limited demineralized flour. The experiments were carried out in triplicate according to the conditions specified in Table 4, using 1.2 g of demineralized flour and 12 mL of NaOH. Once the reactions were completed, the samples were rinsed with hot distilled water until the pH reached a value between 7 and 8. Subsequently, they were placed in an oven at 60 °C overnight, and a protein determination assay via the Micro Kjeldahl method was performed for each sample. The percentage of deproteinization (%DP) was determined by comparing the protein content before and after treatment (Equation (8)), which confirmed the success of protein removal.

$$\%DP = \frac{\text{Protein content before treatment} - \text{Protein content after treatment}}{\text{Protein content before treatment}} \times 100\% \quad (8)$$

Once the battery of experiments was completed, Minitab® Version 19.2020.1.0 was used to analyze the acquired data. This analysis included processing the response surface to generate an ANOVA at a confidence level of 95% ($p < 0.05$). The regression and graphical analysis of the experimental data were fitted using Equation (9) to determine the optimized reaction condition. Where the predicted response is Y and the model constant is β_0 ; the independent variables are x_1 , x_2 , and x_3 ; the linear coefficients are β_1 , β_2 , and β_3 ; the cross-product coefficients are β_{12} , β_{13} , and β_{23} ; and the quadratic coefficients are β_{11} , β_{22} , and β_{33} .

The demineralized cricket flour was deproteinized using the optimized condition and dried at 60 °C in an oven overnight. The next steps involved using this deproteinized flour.

$$Y = \beta_0 + \beta_1x_1 + \beta_2x_2 + \beta_3x_3 + \beta_{12}x_1x_2 + \beta_{13}x_1x_3 + \beta_{23}x_2x_3 + \beta_{11}x_1^2 + \beta_{22}x_2^2 + \beta_{33}x_3^2 \quad (9)$$

2.4. Purification and Bleaching Process

A sample of 5.65 g of deproteinized flour was placed in a flask with 56.5 mL of 1% sodium hypochlorite (J.T. Baker) and left at room temperature with constant stirring for 3 h. Subsequently, it was rinsed with distilled water and left to dry overnight in an oven at 60 °C. The same process was repeated to undergo a second bleaching process. This yielded purified chitin, from which 2.3 g samples were taken for its physicochemical characterization.

2.5. Deacetylation (DA)

A sample of 1 g of purified chitin was mixed with 20 mL of 50% NaOH (Desarrollo de Especialidades Químicas), and the mixture was autoclaved in a Market Forge Sterilmatic® autoclave (Burlington, VT, USA) for three cycles of 45 min at 121 °C and 0.95 kg/cm² of pressure. Once the reaction was complete, the sample was rinsed with distilled water until it reached a neutral pH and then was left to dry overnight in an oven at 60 °C. This chitosan was subsequently used for posterior physicochemical characterization. The DA process was performed in triplicate.

2.6. Physicochemical Characterization Process of Chitin and Chitosan Obtained from *Acheta domesticus* Cricket Flour

Chitin and chitosan are valuable biopolymers for various industries. They underwent physicochemical characterization through different techniques, including those derived for insect sources that closely resemble the cricket species *Acheta domesticus*. Therefore, the characterization of chitin and chitosan samples was conducted using four techniques: Fourier-Transform Infrared Spectroscopy (FTIR) was used for identifying functional groups and X-ray Diffraction (XRD) for determining the crystalline structure. Both techniques aimed to confirm the identity of the compounds. Scanning Electron Microscopy (SEM) was also used, which allows for the determination of the morphology of the polymers, as

well as Differential Scanning Calorimetry (DSC), which elucidates the thermal behavior of the sample in a range of 25 to 250 °C. The purpose of this characterization was to verify that the physicochemical properties are similar to those of commercially available chitin and chitosan.

For the FTIR analysis, a Perkin Elmer Spectrum 400 Spectrophotometer (Waltham, MA, USA) was employed at a resolution of 4 cm⁻¹ and 32 scans. Equation (10) was used to estimate the percentage of deacetylation (%DA) in the chitosan sample, derived from the wave number and absorbance of the carbonyl group of the secondary amide (1655 cm⁻¹) and the hydroxyl group (3257 cm⁻¹) [7].

$$\%DA = 100 - \left[\frac{A_{1655}}{A_{3257}} \right] \times \frac{1}{1.33} \quad (10)$$

The XRD analysis was carried out using a Rigaku MiniFlex 600 diffractometer (Akishima-shi, Tokyo, Japan) under the following conditions: an initial angle of 5°, a final angle of 80°, 0.05° step, and a scanning velocity of 10 degrees/min. The crystallinity index (%CrI) was calculated using Equation (11), where I_c represents the maximum peak intensity for the highest peak (crystalline fraction), and I_a represents the peak with the minimum intensity within the highest peaks (amorphous fraction).

$$\%CrI = [(I_c - I_a)/I_c] \times 100 \quad (11)$$

For the DSC analysis, a PerkinElmer DSC 8000 (Shelton, CT, USA) instrument was used, featuring a heating range of 25 °C to 250 °C and a heating slope of 10 °C/min. Additionally, SEM analysis was conducted using a Phenom ProX microscope (Almelo, OV, The Netherlands) operating at 5 kV, equipped with a backscattered electron detector with a tungsten wire. All graphs were processed using MagicPlot Version 3.0.1 software (Saint Petersburg, Rusia).

3. Results

3.1. Compositional Analysis of Cricket Flour

Table 1 shows the consolidated results for the proximal analysis, which includes the percentages on both wet and dry bases of humidity, fat, ashes, protein, and crude fiber present in the original sample. To determine the total carbohydrate content, the percentage values of humidity, fat, ashes, and protein were subtracted from 100%. These values were then compared with those reported in the scientific literature for *Acheta domesticus* (Table 1).

Humidity determination was conducted to calculate the other constituents of cricket flour on a uniform basis (either dry or wet) [28]. The humidity percentage obtained for the sample (2.55%) was lower than that reported by Udomsil et al. [29] (6.3%) for the cricket species *Acheta domesticus*.

Table 1. Proximal analysis for *Acheta domesticus* cricket flour.

Analysis	* Wet Base (%)	* Dry Base (%)	** Reported Values for <i>Acheta domesticus</i> (%)
Humidity	2.55 ± 0.11	-	6.3 ± 0.04
Fat	13.01 ± 0.65	13.35 ± 0.65	10.4 ± 0.1
Ashes	4.19 ± 0.04	4.30 ± 0.04	5.4 ± 0.3
Protein	54.85 ± 0.69	56.29 ± 0.69	71.7 ± 0.5
Crude fiber	15.31 ± 1.01	15.71 ± 1.01	4.6 ± 0.2
Carbohydrates	25.40	26.06	1.6

* Values from this study; ** Udomsil et al. [29]. Percentages on a dry basis.

Ashes determine the quantity of minerals that are present in a sample, which is important to know as a reference point to compare after the DM process has been carried out. A value of 4.3% was similar to that reported in the literature of 5.4% for the house cricket [29].

The determined fat content in this case was 13.35%, which is higher than the value reported by Udomsil et al. [29]. However, the differences in these values can be attributed to variations in experimental methods. Udomsil et al. [29] employed a chloroform/methanol solvent, followed by a transesterification treatment with methanolic KOH, and identified fat components using gas chromatography analysis. In contrast, this project does not involve such a detailed analysis of the starting raw material; therefore, gravimetric analysis was chosen as the preferred method.

The protein content in cricket flour was found to be high. However, it is important to note that this value might overestimate the amount of nitrogen from amino acids due to the conversion factor for nitrogen quantity. Insects, including crickets, contain significant amounts of non-protein nitrogenated compounds such as chitin. To address this issue, we used a reference conversion factor of 5.25, as reported by Boulos et al. [30] for the species *Acheta domesticus*. The calculated protein value was 56.29 g, and the use of the nitrogen quantity conversion factor may account for the observed difference between our result and the protein content reported by Udomsil et al. [29]. Their reported protein content was 71.7% using a conversion factor of 6.25.

Crude fiber refers to the organic, non-nitrogenated substances that do not dissolve during subsequent acid or alkaline hydrolysis. Therefore, fiber can be reported as part of carbohydrates. In this case, cricket flour was found to have 26.06% carbohydrates (dry base), of which 60.28% was crude fiber, constituting 15.71% of the total composition of the cricket flour sample. In comparison, Udomsil et al. [29] reported values of 4.6% for fiber and 1.6% for carbohydrates. This discrepancy can be explained by the fact that these authors did not consider fiber as part of carbohydrates, and the amount of protein was likely overestimated due to the high value of the conversion factor used (6.25).

3.2. Standardization of DM Process

A Tukey test was performed, revealing that experimental conditions 1, 3, 7, and 8 exhibited statistical equality and included the highest %DM values, marked in bold (Table 2). Among these conditions, number seven was selected (HCl concentration 2 M at 30 °C for 3 h) since it represents the shortest reaction time and the lowest reaction temperature. This choice renders the process more environmentally friendly and less energetically costly without statistically impacting the %DM.

Table 2. Experimental conditions and results of DM process for *Acheta domesticus* cricket flour.

Experimental Condition	HCl Concentration (M)	Time (h)	Temperature (°C)	* Ash Content (%)	* %DM
1	1	6	65	0.37 ± 0.03	92.1 ± 0.69 A,B,C,D
2	1	3	30	0.47 ± 0.05	90.09 ± 0.98 B,C,D,E
3	2	3	65	0.29 ± 0.11	93.86 ± 2.34 A
4	1	3	65	0.53 ± 0.05	88.84 ± 1.08 D,E
5	1	6	30	0.62 ± 0.06	86.79 ± 1.27 E
6	2	6	30	0.49 ± 0.03	89.56 ± 0.59 C,D,E
7	2	3	30	0.36 ± 0.03	92.25 ± 0.67 A,B,C
8	2	6	65	0.33 ± 0.04	93.02 ± 0.92 A,B

* Results are the mean value of a triplicate, ± standard deviation. Mean values with different superscripts indicate statistical differences (Tukey test, 95% confidence).

Table 2 displays the results of DM experiments conducted to standardize this process. The %DM was calculated by comparing the ash content with the initial value in the proximal analysis (4.3%). A significant decrease in mineral content can be observed under all experimental conditions, with values ranging 86.79% to 93.86% for %DM.

Considering the obtained results, an ANOVA was conducted, revealing that the temperature and HCl concentration factors were statistically significant ($p < 0.05$), whereas the reaction time was not (Table 3). It was determined that a concentration of HCl at 2 M and a temperature of 65 °C represent the levels that maximize the %DM, corresponding to

experimental conditions 3 and 8. Condition number 8 was excluded due to the observation of an unfavorable reaction in the sample (manifested as a black and viscous appearance), suggesting potential protein denaturation or alteration to the chitin structure.

Table 3. ANOVA test for %DM.

Factor	Degree of Freedom	Sum of Square	Mean Square	F-Value	p-Value ($\alpha = 0.05$)
Time	1	4.788	4.788	1.53	0.230
Temperature	1	31.190	31.190	10.00	0.005
HCl Concentration	1	44.366	44.336	14.21	0.001

Finally, the condition that maximizes the %DM was implemented to demineralize the previously degreased cricket flour. Samples were taken to perform ash determination to verify the maximization of the %DM, and the result was $95.85 \pm 0.012\%$.

3.3. Optimization of Deproteinization Process

Table 4 displays the conditions and results of the Box–Behnken design experiments to optimize the DP process. The percentage of protein (dry weight) was used to calculate the %DP, with values ranging from 27.13 to 52.61.

Table 4. Experimental conditions and results for DP process optimization for *Acheta domesticus* cricket flour according to Box–Behnken design.

Experimental Condition	NaOH Concentration (M)	Time (min)	Temperature (°C)	* Protein (%)	* %DP
1	3	45	70	30.67 ± 3.63	44.08 ± 6.44
2	2	30	70	25.99 ± 1.84	52.61 ± 3.27
3	2	45	80	30.3 ± 0.08	44.76 ± 0.14
4	2	15	80	34.15 ± 0.3	37.73 ± 0.53
5	1	30	60	38.57 ± 1.69	29.69 ± 3.00
6	2	30	70	36.69 ± 2.11	33.11 ± 3.75
7	1	30	80	34.64 ± 0.31	36.84 ± 0.54
8	1	15	70	39.97 ± 0.88	27.13 ± 1.56
9	3	15	70	32.27 ± 1.97	41.16 ± 3.50
10	3	30	60	34.39 ± 0.97	37.31 ± 1.73
11	1	45	70	35.32 ± 0.72	35.6 ± 1.27
12	3	30	80	32.13 ± 2.88	41.42 ± 5.11
13	2	15	60	34.22 ± 0.38	37.62 ± 0.68
14	2	30	70	33.54 ± 4.07	38.84 ± 7.22
15	2	45	60	31.43 ± 2.98	42.7 ± 5.30

* Results for protein (%) and %DP are the mean of value of triplicate experiments, \pm standard deviation.

After conducting the 15 experiments in triplicate, a statistical analysis of the data was performed using a Box–Behnken surface response model in MINITAB® Version 19.2020.1.0 software. The resulting ANOVA used the %DP as the response variable, as depicted in Table 5. The analysis revealed that reaction time, NaOH concentration, and the concentration*concentration interaction were significant factors affecting the response variable. The regression equation for the model was determined (Equation (12)), where C represents the concentration of NaOH (M), T is temperature of the reaction (°C), and t is the reaction time (minutes). Next, a prediction of the optimal conditions to maximize the %DP value was performed, resulting in the following parameters: 80 °C for temperature, 45 min for reaction time, and 2.56 M for NaOH concentration. The %DP was predicted to reach $46.37 \pm 3.86\%$ with a 95% confidence interval, using the optimal established conditions.

$$\% \text{ DP} == -3.84 C^2 + 19.70 C + 0.17 T + 0.197 t - 1.33 \quad (12)$$

Table 5. ANOVA test for %DP.

Factor	Degree of Freedom	Sum of Square	Mean Square	F-Value	p-Value ($\alpha = 0.05$)	Determination Coefficient (R^2)
Temperature	1	65.87	65.87	2.54	0.119	86.13
Time	1	199.97	199.97	7.70	0.009	
Concentration OH	1	451.8	451.80	17.40	0.000	
(Concentration OH)	1	156.00	156.00	6.01	0.019	
(Concentration OH)	1					

The experimental value of the optimal condition was determined in triplicate to validate the %DP predicted by the model, yielding a value of $43.23 \pm 1.25\%$. This value falls within the predicted confidence interval.

3.4. Chitin Bleaching

An amount of 5.3 g of bleached purified chitin was obtained. It is noticeable that the color becomes lighter after each whitening treatment (Figure 1).

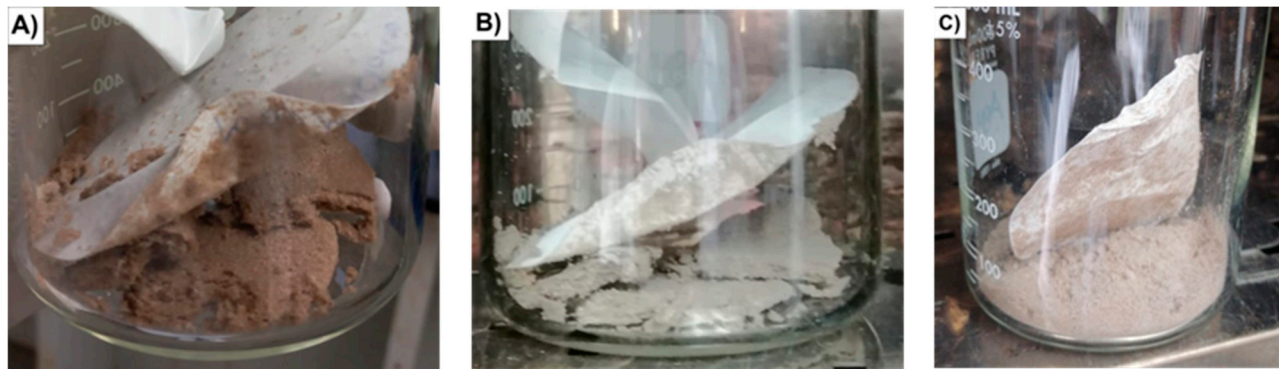


Figure 1. Bleaching process showing chitin pre bleaching treatment (A), chitin after first bleaching treatment (B), and chitin after second bleaching treatment (C).

3.5. % DA of Chitin and Obtention of Chitosan

After the DA process of the chitin, chitosan was obtained. The %DA was calculated using Equation (10), considering the IR bands present at 1645 cm^{-1} from the carbonyl group in the secondary amine and at 3237 cm^{-1} corresponding to the hydroxyl group of the chitosan FTIR spectrum. A DA degree of 99.47% was achieved, and the presence of chitosan can be observed in the FTIR spectrum (Section 4.4).

3.6. Characterization of Chitin and Chitosan Extracted from *Acheta domesticus* Cricket Flour

Regarding the FTIR analysis, all bands were identified and corresponded to the characteristic functional groups of chitin and chitosan, including alcohols, amides, amines, carbonyl groups, and ethers. Also, the peaks in the XRD analysis coincided with those reported in the scientific literature (9.1° and 19.3° for chitosan at 9.1° and 19.1° in 2θ). Additionally, the SEM images also exhibited similar features to other analyzed samples of related cricket species. Finally, the DSC analysis provided supporting evidence for the correct identification of both compounds, as indicated by the presence of exothermic peaks and the absence of endothermic peaks. These results will be further elucidated in the Discussion section.

4. Discussion

4.1. Compositional Analysis of Cricket Flour

The compositional analysis results obtained from the *Acheta domesticus* cricket flour differed from those reported by Udomsil et al. [29]. Regarding the ash content, the difference

in values could be attributed to the sample drying time, which was 24 h at 100 °C for the cricket flour used in our study, while Udomsil et al. [29] reported a 6 h drying time at 105 °C. Additionally, the discrepancy may arise from the storage conditions of the samples before the dehydration process and the method implemented to determine the ash content. Our study employed a gravimetric method with furnace calcination at 900 °C, in contrast to the official food method's recommendation of 500 °C [31]. Initially, two trials were conducted at 500 °C, but they proved unsuccessful as the ashes appeared gray instead of white, and the ash percentage was too high (10.16%). Subsequent exploration of the scientific literature revealed the presence of calcium carbonate in cricket flour, a compound challenging to fully calcinate at 500 °C given its occurrence in insect exoskeletons [6,32]. Consequently, the temperature was increased to 900 °C to ensure complete calcination. On the other hand, Udomsil et al. [29] employed a different method. They used microwave digestion with hydrochloric acid and Inductively Coupled Plasma–Optical Emission Spectroscopy (ICP-OES) to quantify the minerals present in a more specific way, a technique that was beyond the scope of this study. Finally, the nutritional composition of crickets is closely linked to their maturity stage and diet [33], factors that could account for the variations in the remaining composition percentages presented in Table 1.

4.2. Standardization of DM Process

Regarding the obtained results for the DM process, condition number seven was shown to be the one that maximized the %DM without compromising the environmental impact of the process (HCl concentration 2 M at 30 °C for 3 h). This is supported by the ANOVA performed, whose results are shown in Table 3. Considering a significance level of 0.05, it can be observed that the statistically significant factors affecting the %DM are the reaction temperature and the concentration of HCl. This is evident from their lower values in comparison to the alpha value, which were considered when determining the set of results for selection in the Tukey test.

The %DM is not commonly reported in the scientific literature. However, Psarinos et al. [34] published a %DM of $91.1 \pm 0.3\%$ using 1 M HCl for 2 h at 98 °C for house crickets, in comparison to the $95.85 \pm 0.012\%$ achieved in our study. Based on these results, it can be concluded that a successful standardization of the DM process was achieved.

4.3. Optimization of DP Process

Based on the obtained results, the Box–Behnken model successfully optimized the deproteinization process to maximize the %DP. This is supported by the ANOVA results presented in Table 5. The ANOVA identified key factors influencing %DP, namely, reaction temperature, time, NaOH concentration, and concentration*concentration interaction. However, there was a significantly low yield of solids during the DP stage, obtaining 14.12% of unpurified chitin from the demineralized flour. This value cannot be directly compared to those reported in the scientific literature because it does not consider the original composition of the flour. However, it is noteworthy that the yields for chitin extraction are generally low, ranging from 2.5% to 12.2% in both insects and crustaceans [35].

The %DP reflects a significant quantity of nitrogen left in the sample after DP. It is important to highlight that the Micro Kjeldahl method, employed for total nitrogen content quantification in the sample, does not exclusively measure amino acid-derived nitrogen. Chitin and chitosan, unlike proteins, are nitrogen-containing carbohydrates that exhibit fiber-like properties without being derived from vegetable sources. This characteristic might lead to an overestimation of the %DP, as it includes nitrogen from these non-protein structures, even after significant protein removal. Previously, we mentioned the possibility of using a specific nitrogen conversion factor for *Acheta domesticus* that accounts for these non-protein nitrogenated structures. However, in a deproteinized sample, the remaining nitrogen present is very unlikely to come from amino acids since the nitrogen conversion factor does not consider the atypically lower protein content for this species. Additionally,

no comparative studies reporting %DP were found, limiting our ability to compare our findings with the existing scientific literature.

Furthermore, the acid hydrolysis step in demineralization may produce hydrochlorated glucosamine (GlcHCl) in small quantities, potentially increasing the total nitrogen detected by the Micro Kjeldahl method in the cricket flour samples after DP [36]. Additionally, the presence of N-acetylglucosamine, a compound that forms when chitin is exposed to highly acidic environments (like those induced by HCl), inversely affects the crystallinity index and reduces the degree of acetylation. These impacts were considered during the characterization stage as detailed in Sections 4.5 and 4.7 [37,38].

In our experiments, the NaOH concentration was adequately strong, and the reaction time was sufficient across all experimental conditions to ensure efficient DP. This is in line with the literature reporting that the concentration of alkaline solutions for protein removal in diverse crustacean and arthropod samples typically ranges from 0.025 to 4 M of a strong base (generally NaOH). These studies have utilized temperatures ranging from 25 °C to 150 °C reaction times from 20 min to 96 h. Such conditions have been shown to yield 1.79% to 7.1% of chitin and chitosan, respectively, in cricket (*Gryllus bimaculatus* and *Brachytrupes portentosus*) samples [35].

4.4. Characterization: Identification of Chitin and Chitosan's Functional Groups Using FTIR

FTIR analyzes how matter interacts with infrared radiation, enabling the identification of chemical species by determining the frequencies at which different functional groups absorb in the IR spectra [39]. This technique effectively confirms the presence of both chitin and chitosan as it identifies their characteristic functional groups in the spectra. These include alcohols, amides (found in chitin), amines (in chitosan), carbonyl groups, and ethers, appearing at wavelengths of 3650 cm⁻¹, 1640 cm⁻¹, 3500 cm⁻¹, 1700 cm⁻¹, and ~1100 cm⁻¹, respectively [3,40,41].

Figure 2 shows the FTIR spectrum of whitened chitin obtained under the standardized and optimized conditions DM and DP, as outlined in previous sections. The spectrum clearly reveals the presence of all functional groups characteristic of chitin's structure. A broad band at 3434 cm⁻¹ indicates the stretching of the hydroxyl group (-OH), while a more intense band at 3256 cm⁻¹ indicates the stretching of the -NH group, associated with a secondary amide, typical of chitin. Additionally, lower intensity bands at 3097 and 2876 cm⁻¹ correspond to the stretching of the -CH and -CH₃ groups, respectively. The medium intensity bands near 1645 cm⁻¹, attributed to carbonyl group C=O stretching, confirm the α (alpha) crystalline structure of the chitin obtained. This identification is because chitin exists in three crystalline structures in nature: α -chitin, with two bands around 1650 cm⁻¹; β -chitin, showing a single band at 1650 cm⁻¹; and γ -chitin, for which not much information can be found in the scientific literature [3,42].

A medium-intensity band at approximately 1551 cm⁻¹ in the FTIR spectrum corresponds to the bending of the -NH group and the stretching of the C-N bond. Notably, the absence of a band around 1540 cm⁻¹ in this region indicates successful DP. A signal in this wave number typically indicates the presence of peptide bonds. Its absence therefore implies a minimal presence of proteins in the whitened chitin (Figure 2) [43]. The next band, at around 1375 cm⁻¹, shows a bending of the hydroxyl group bond (-OH), verifying its presence in the obtained compound as it complements the band at 3434 cm⁻¹ (Figure 2). Finally, intense bands can be seen at 1067, 1010, and 720 cm⁻¹ in the fingerprint region, corresponding to the stretching of the C-OH bond of the primary alcohol, the stretching of the C-O bond corresponding to the cyclic 5-carbon ether, and the bending of the N-H bond of the amide group, respectively, further delineating the molecular structure of chitin (Figure 2).

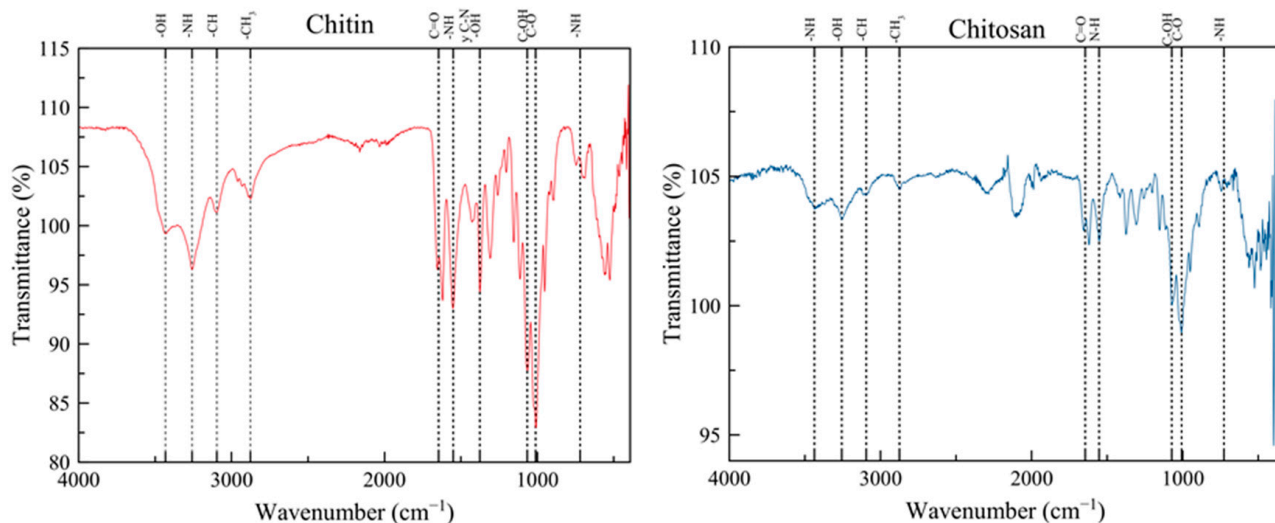


Figure 2. IR spectrum of chitin (**left**) and chitosan (**right**) extracted from *Acheta domesticus* crickets showing its characteristic and dominant functional groups.

The chitosan obtained from the whitened chitin showed notable differences with the chitin IR spectrum, as shown in Figure 2 on the right side. A difference is the band at 3437 cm^{-1} , which corresponds to the stretching of the -NH bond in the primary amine, a feature of the molecular structure of chitosan following the DA process of chitin. Additionally, the band at 3257 cm^{-1} is indicative of the hydroxyl group bond (-OH) stretching similar to that in chitin. Lower intensity bands at 3095 and 2876 cm^{-1} represent the stretching of the -CH and -CH₃ groups, respectively. Carbonyl group stretching is observed at 1645 cm^{-1} and the bending of the -NH bond, characteristic of an amine, appears around 1555 cm^{-1} (Figure 2). These bands are typical in IR spectra for chitosan as it is not completely deacetylated. Therefore, the presence of a carbonyl group in the IR spectrum depends on the degree of DA of the chitosan in the sample [8].

Since the degree of DA obtained was 99.47%, it can be considered that the time and conditions under which the DA process was performed were extremely efficient. This result is comparable to those reported for chitin DA from other insect sources such as silkworm *Bombyx mori*, in which 94% was obtained using NaOH 40% for 4 h at $110\text{ }^{\circ}\text{C}$ [35]. The results agree with reports where it is stated that the DA of insects' chitin is easier than that of chitin from crustaceans. There are reports of only 75% for samples extracted from *P. monodon* shrimps using HCl 1 M at $25\text{ }^{\circ}\text{C}$ for DM, NaOH 1 M at $100\text{ }^{\circ}\text{C}$ for 8 h for DP, and NaOH 50% at $100\text{ }^{\circ}\text{C}$ for 8 h for DA [35].

Finally, Figure 3 shows the differences in the bands present in the chitin and chitosan that were obtained in this study (chitin E and chitosan E) in comparison to the commercially available chitin and chitosan extracted from crab (chitin C and chitosan C) reported by Sáenz et al. [44].

The stretching bands of the hydroxyl group -OH and the -NH bond around 3500 cm^{-1} and 3450 cm^{-1} , respectively, are slightly more intense in the experimental chitin. However, both samples show the characteristic bands of the functional groups, with similar intensities between them, including the C=O bond stretch around 1645 cm^{-1} ; the bending of the N-H bond and the stretching of the C-N bond of the secondary amide around 1551 cm^{-1} ; the stretching of the -CH and -CH₃ bonds that are visible around 3097 and 2876 cm^{-1} , respectively; the stretching of the C-OH bond of the primary alcohol at 1067 cm^{-1} ; the stretching of the C-O group corresponding to the 5-carbon cyclic ether at 1010 cm^{-1} ; and the bending of the -NH bond in the amide group around 720 cm^{-1} .

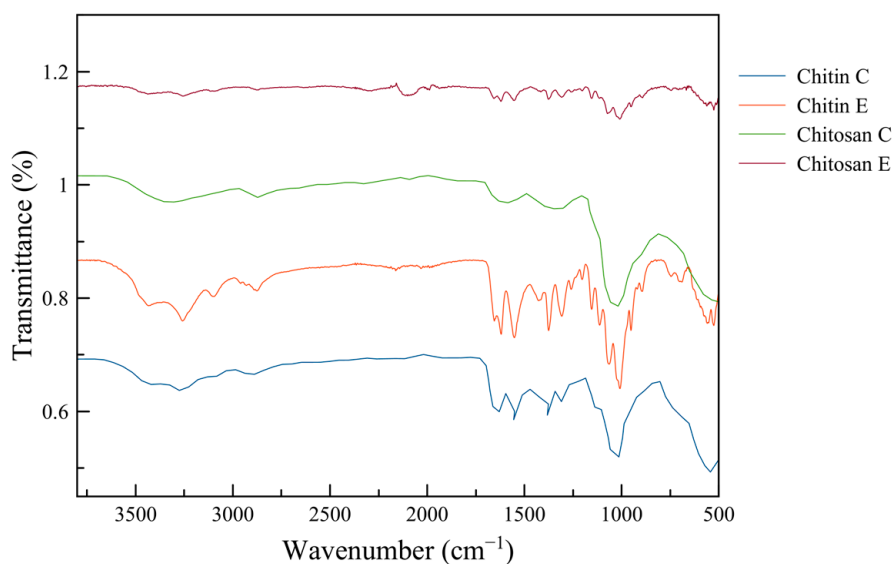


Figure 3. IR spectra of chitin E and chitosan E extracted from *Acheta domesticus* cricket flour in comparison to commercially available chitin C and chitosan C reported by Sáenz et al. [44].

On the other hand, the IR spectrum for the chitosan from this work and commercial chitosan differ from each other mainly in the intensity and clarity of the characteristic bands. Nevertheless, the main functional groups can be distinguished, such as the -NH and -OH bond stretching bands at around 3400 and 3300 cm^{-1} , respectively; the stretching of the C=O bond (1645 cm^{-1}); the bending of the primary amine N-H bond (1555 cm^{-1}); and the stretching of the C-O bond corresponding to the 5-carbon cyclic ether at around 1009 cm^{-1} .

Because of the great similarity between the IR spectra for chitin and chitosan from this work and the commercial reference, it can be stated that we successfully obtained these polysaccharides from *Acheta domesticus* in accordance with the conditions established in this study [44].

4.5. Characterization: Identification of Chitin and Chitosan's Crystalline Structure Using XRD

XRD is an analytical technique that measures the diffraction that an X-ray shows when it interacts with the atoms of a sample. It is especially useful to identify the crystalline structure and the purity of a sample without extensive sample preparation [45]. In previous studies, XRD showed distinctive peaks for chitin at 9.1° and 19.3° and for chitosan at 9.1° and 19.1° in 2θ , where it is possible to identify three crystalline forms of chitin (α , β , and γ) based on the presence of hydrogen bonds in its structure [4].

The result is a diffractogram that shows the diffraction angle of the X-ray in 2θ and the intensity of the received signal when diffracting occurs when the X-ray encounters the chitin and chitosan. As well, it allows the identification of the crystallographic planes and the crystalline network of both compounds [45,46].

Figure 4 shows the XRD analysis results for chitin and chitosan obtained in this study from *Acheta domesticus* cricket flour compared to commercially available chitin and chitosan extracted from crab reported by Escobar et al. [14]. These diffractograms show the most representative peaks for commercial chitin and chitosan, which match, in shape and position, those found in the samples obtained in this report, confirming the identity of the compounds. Additionally, the crystalline peaks around 9.6 , 19.6 , 21.1 , and 23.7 degrees in 2θ confirm that the obtained chitin is α -chitin, as previously reported in other publications. This observation demonstrates that the crystalline form obtained aligns with the most commonly obtained form of chitin from crustaceans available in the industry [47,48].

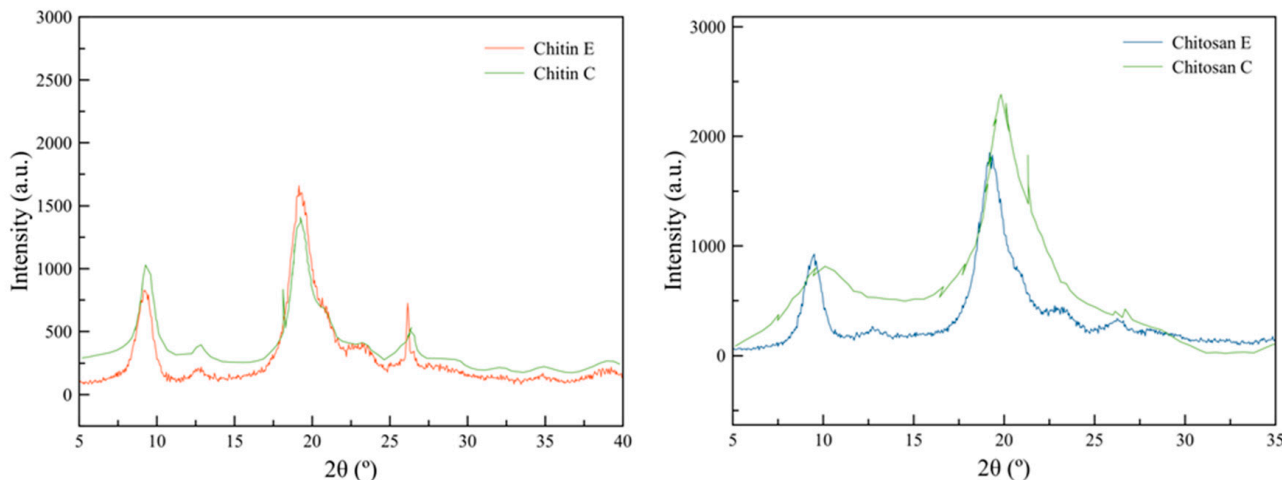


Figure 4. Obtained XRD diffractograms for chitin and chitosan obtained in this study (chitin E and chitosan E) from *Acheta domesticus* cricket flour in comparison to results reported by Escobar et al. [14] using XRD on commercially available chitin and chitosan obtained from crab (chitin C and chitosan C).

The crystallinity index was also calculated for the samples, resulting in 93.86% and 90.60% for chitin and chitosan, respectively. In comparison, 81.84% and 58.14% were reported for commercially available chitin and chitosan. It has been reported that the crystallinity indexes for chitin vary from 83.4% to 85.21% and from 50.1% to 49.1% for chitosan extracted from grasshopper and shrimp husk sources, respectively [7,48]. A higher crystallinity index represents a higher thermal stability of the compounds, as it indicates the presence of a minimum quantity of amorphous regions in the samples and therefore the premature degradation of its structure at high temperatures can be avoided (Section 4.7).

4.6. Morphology of Chitin and Chitosan Using SEM

SEM is a characterization technique that uses an electron beam instead of a beam of light to form an amplified image. It is used to perform topographical, structural, and compositional analysis. The image obtained is the response of the material to the impact of the electron beam; in other words, it is the reflection of the beam [49]. SEM images taken from previous studies show fibrous and laminar structures for chitin obtained from the cricket *Brachystola magna*, while a fibrillar lattice is observed for the subsequent chitosan [4].

Figure 5 shows the SEM image obtained for the chitin extracted from *Acheta domesticus* cricket flour in the upper row. It is possible to identify a fibrous morphology, as well as lattice, linear, and fibrous structures in its composition that confirm the crystalline structure of the compound, especially when compared to the results obtained by Monter-Miranda et al. [4]. The small and dispersed dark spots in the fibers can be attributed to the degradation of the chitin. To increase the conductivity of the sample, the chitin was covered in gold, causing the impact of a larger number of electrons that magnified the image, but caused an increase in the temperature of the sample, resulting in partial degradation of the polymer.

Figure 5 also shows the SEM images obtained for the chitosan extracted from *Acheta domesticus* cricket flour in the lower row. Fibrillar structures similar to those present in chitin can be seen (Figure 5; upper row), which coincide with the images reported by Monter-Miranda et al. [4], and this confirms the presence of chitosan. This sample showed no dark spots, which could be because this sample was not treated with a gold coating for SEM observation in order to prevent sample degradation; however, the chitosan image was of lower detail in comparison with the chitin image (Figure 5).

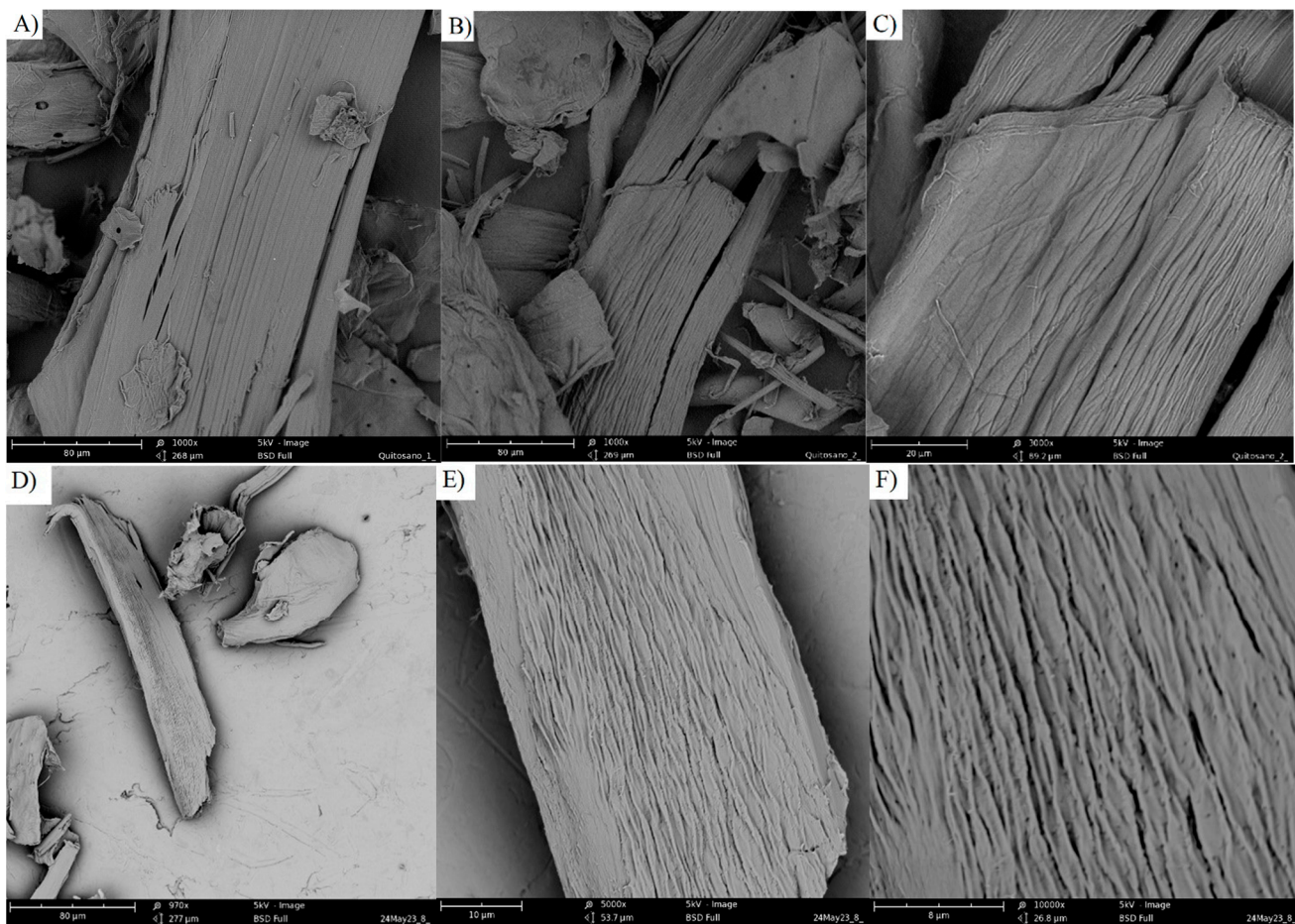


Figure 5. SEM images of chitin extracted from *Acheta domesticus* cricket flour (upper row) with a 970x (A), 5000x (B), and 10,000x (C) close-up and of chitosan extracted from *Acheta domesticus* cricket flour (lower row) with a 1000x (D,E) and 3000x (F) close-up.

4.7. Characterization: Analysis of Chitin and Chitosan's Thermal Behavior Using DSC

DSC was used to find the thermic stability and transition temperatures of the extracted chitin and chitosan. There are no DSC studies for these molecules from sources similar to *Acheta domesticus* [7,48].

Figure 6 shows the thermogram obtained by DSC of the chitin and chitosan obtained from cricket flour. In the case of chitin, no peak or slope can be perceived, which may indicate the crystallization temperature or the glass transition temperature of the material. The crystallinity index of the chitin is very high and without the presence or scarce presence of amorphous regions, making the thermal behavior of the polymer very stable under high temperatures. It is estimated that changes in chitin's structure may occur when surpassing 300 °C due to decomposition of residual monomers of N-acetyl glucosamine and N-glucosamine [50]. An exothermic peak would be expected around 110 to 160 °C corresponding to water on the polymer chain [50,51]; however, since the sample was previously dried for its analysis, this could not be appreciated in the thermogram.

The chitosan thermogram shows an exothermic peak at 185 °C corresponding to the crystallization temperature (T_c). Similar to chitin, it was expected that a significant exothermic peak may appear at 110 to 160 °C corresponding to water present in the polymer chains; this peak was visible at low intensity at around 140 °C [50,51]. The thermal behavior of chitosan is consistent with its crystalline structure. It has been reported in the scientific literature that this molecule presents a lower crystallinity index than chitin, as observed in the present study, which means that it contains more amorphous regions that turn crystalline when reaching the T_c . Therefore, chitosan is a more reactive chemical

compound than chitin and consequently has a wider variety of applications (biomedicine, cosmetics, residual water treatment, etc.), being a highly sought-after compound in different industries [50,51].

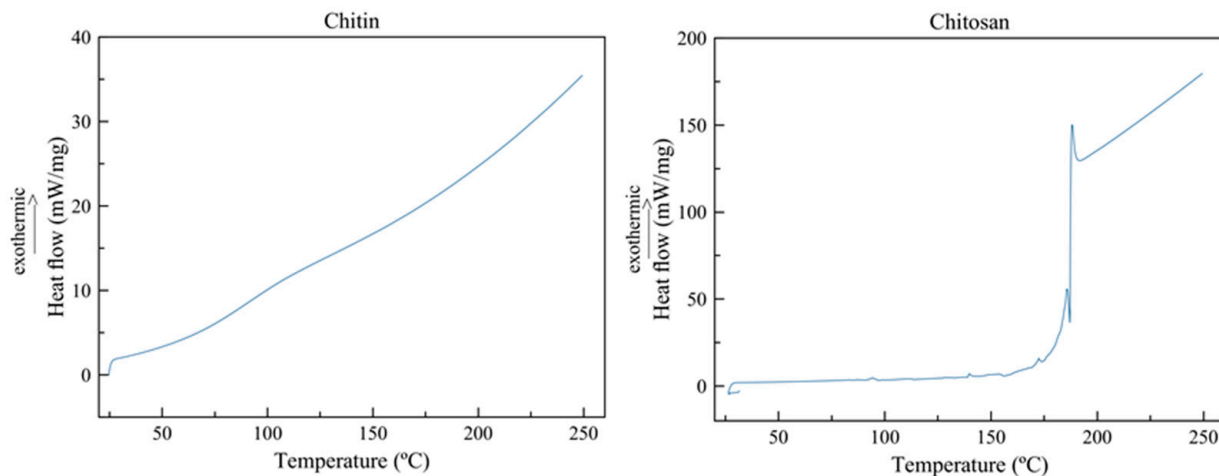


Figure 6. DSC thermogram for chitin and chitosan extracted from *Acheta domesticus* cricket flour.

5. Conclusions

In this study, we succeeded in establishing conditions that maximize and optimize the DM and DP of *Acheta domesticus* chitin. The maximum %DM and %DP were 95.85% and 43.23%, respectively. The identity and physicochemical characteristics of the chitin and chitosan produced were confirmed using FTIR, XRD, SEM, and DSC analyses. These results could be adopted for chitin extraction from other insects instead of using conditions established for crustaceans. Additionally, future studies are required to investigate the applications (such as antimicrobial activity, prebiotic effects, and plant bio-stimulation) of chitin obtained from insects using the conditions established in this study.

Author Contributions: Conceptualization, L.R.-S. and C.C.-H.; methodology, A.E.-S., A.V.-S. and C.L.-R.; validation, L.R.-S., C.C.-H. and L.M.M.; formal analysis, A.E.-S., A.V.-S. and C.L.-R.; investigation, A.E.-S., A.V.-S. and C.L.-R.; resources, C.C.-H.; data curation, L.R.-S. and C.C.-H.; writing—original draft preparation, A.E.-S.; writing—review and editing, L.R.-S., C.C.-H. and L.M.M.; visualization, A.E.-S.; supervision, L.R.-S., C.C.-H. and L.M.M.; project administration, L.R.-S. and C.C.-H.; funding acquisition, C.C.-H. All authors have read and agreed to the published version of the manuscript.

Funding: This research received no external funding.

Data Availability Statement: The data presented in this study are available from the corresponding author on reasonable request.

Acknowledgments: We would like to thank Juan Pablo Dávila, Aidee Sánchez, and Sergio Serna for their support in providing the necessary space, resources, and guidance for the duration of this study.

Conflicts of Interest: The authors declare no conflicts of interest.

References

- Knidri, H.E.; Belaabed, R.; Addaou, A.; Laajeb, A.; Lahsini, A. Extraction, chemical modification and characterization of chitin and chitosan. *Int. J. Biol. Macromol.* **2018**, *120*, 1181–1189. [[CrossRef](#)]
- Iber, B.T.; Kasan, N.A.; Torsabio, D.; Omuwa, J.W. A review of various sources of chitin and chitosan in nature. *J. Renew. Mater.* **2022**, *10*, 1097–1123. [[CrossRef](#)]
- Mohan, K.; Ganesan, A.R.; Muralisankar, T.; Jayakumar, R.; Sathishkumar, P.; Uthayakumar, V.; Revathi, N. Recent insights into the extraction, characterization, and bioactivities of chitin and chitosan from insects. *Trends Food Sci. Technol.* **2020**, *105*, 17–42. [[CrossRef](#)]
- Monter-Miranda, J.G.; Tirado-Gallegos, J.M.; Zamudio-Flores, P.B.; Rios-Velasco, C.; Ornelas-Paz, J.D.J.; Salgado-Delgado, R.; Hernández-Centeno, F. Extracción y caracterización de propiedades fisicoquímicas, morfológicas y estructurales de quitina y quitosano de *Brachystola magna* (Girard). *Rev. Mex. Ing. Quim.* **2016**, *15*, 749–761. [[CrossRef](#)]

5. Kumari, S.; Kishor, R. Chitin and chitosan: Origin, properties, and applications. In *Handbook of Chitin and Chitosan*, 1st ed.; Gopi, S., Thomas, S.P., Eds.; Elsevier: Amsterdam, The Netherlands, 2020; pp. 1–33.
6. Hahn, T.; Tafi, E.; Paul, A.; Salvia, R.; Falabella, P.; Zibek, S. Current state of chitin purification and chitosan production from insects. *J. Chem. Technol. Biotechnol.* **2020**, *95*, 2775–2795. [[CrossRef](#)]
7. Luo, Q.; Wang, Y.; Han, Q.; Ji, L.; Zhang, H.; Fei, Z.; Wang, Y. Comparison of the physicochemical, rheological, and morphologic properties of chitosan from four insects. *Carbohydr. Polym.* **2019**, *209*, 266–275. [[CrossRef](#)] [[PubMed](#)]
8. Kaya, M.; Bağrıaçık, N.; Seyyar, O.; Baran, T. Comparison of chitin structures derived from three common wasp species (*Vespa crabro* Linnaeus, 1758, *Vespa orientalis* Linnaeus, 1771 and *Vespula germanica* (Fabricius, 1793)). *Arch. Insect Biochem. Physiol.* **2015**, *89*, 204–217. [[CrossRef](#)] [[PubMed](#)]
9. Kaya, M.; Bitim, B.; Mujtaba, M.; Koyuncu, T. Surface morphology of chitin highly related with the isolated body part of butterfly (*Argynnis pandora*). *Int. J. Biol. Macromol.* **2015**, *81*, 443–449. [[CrossRef](#)]
10. Amoo, K.O.; Olafadehan, O.A.; Ajayi, T.O. Optimization studies of chitin and chitosan production from Penaeus notialis shell waste. *Afr. J. Biotechnol.* **2019**, *18*, 670–688.
11. Ovando, E.; Rodríguez-Sifuentes, L.; Martínez, L.M.; Chuck-Hernández, C. Optimization of soybean protein extraction using by-products from NaCl electrolysis as an application of the industrial symbiosis concept. *Appl. Sci.* **2022**, *12*, 3113. [[CrossRef](#)]
12. Dar, M.A.; Kaushik, G. Optimization of process parameters for biodegradation of malathion by *Micrococcus aloeverae* MAGK3 using taguchi methodology and metabolic pathway analysis. *Biocatal. Agric. Biotechnol.* **2022**, *42*, 102362. [[CrossRef](#)]
13. Lahiri, D.; Nag, M.; Sarkar, T.; Dutta, B.; Ray, R.R. Antibiofilm activity of α -amylase from *Bacillus subtilis* and prediction of the optimized conditions for biofilm removal by response surface methodology (RSM) and artificial neural network (ANN). *Appl. Biochem. Biotechnol.* **2022**, *193*, 1853–1872. [[CrossRef](#)] [[PubMed](#)]
14. Sierra, D.M.E.; Orozco, C.P.O.; Rodríguez, M.A.Q.; Villa, W.A.O. Optimización de un protocolo de extracción de quitina y quitosano desde caparazones de crustáceos. *Sci. Tech.* **2013**, *18*, 260–266.
15. Tokath, K.; Demirdöven, A. Optimization of chitin and chitosan production from shrimp wastes and characterization. *J. Food process. Preserv.* **2018**, *42*, e13494. [[CrossRef](#)]
16. Gîjiu, C.L.; Isopescu, R.; Dinculescu, D.; Memecică, M.; Apetroaei, M.R.; Anton, M.; Rău, I. Crabs marine waste—A valuable source of chitosan: Tuning chitosan properties by chitin extraction optimization. *Polymers* **2022**, *14*, 4492. [[CrossRef](#)] [[PubMed](#)]
17. Dinculescu, D.; Gîjiu, C.L.; Apetroaei, M.R.; Isopescu, R.; Rău, I.; Schröder, V. Optimization of chitosan extraction process from *Rapana venosa* egg capsules waste using experimental design. *Materials* **2023**, *16*, 525. [[CrossRef](#)] [[PubMed](#)]
18. Pădurețu, C.C.; Isopescu, R.D.; Gîjiu, C.L.; Rău, I.; Apetroaei, M.R.; Schröder, V. Optimization of chitin extraction procedure from shrimp waste using Taguchi method and chitosan characterization. *Mol. Crys. Liq. Crys.* **2019**, *695*, 19–28. [[CrossRef](#)]
19. Dong, F.; Qiu, H.; Jia, S.; Dai, C.; Kong, Q.; Xu, C. Optimization of extraction of chitin from *procambiarus clarkia* shell by Box-Behnken design. In *E3S Web of Conferences, Proceedings of the 4th International Conference on Energy Materials and Environment Engineering (ICEMEE 2018)*, Zhuhai, China, 28–30 September 2018; EDP Science: Les Ulis, France, 2018; Volume 38, p. 02010.
20. AOAC Official Method 934.06; Moisture in Dried Fruits. AOAC International: Rockville, MD, USA, 1996.
21. AOAC 923.03 Ashes. Available online: <https://law.resource.org/pub/us/cfr/ibr/002/aoac.methods.1.1990.pdf> (accessed on 25 November 2023).
22. AACC. *International Approved Methods of the American Association of Cereal Chemists*; Minnesota University Press: St. Paul, MN, USA, 2000.
23. AOAC Official Method 984.13; Protein (Crude) in Animal Feed and Pet Food. AOAC International: Rockville, MD, USA, 1996.
24. NOM-Y-118-A-1982 Determinación de Proteína. Available online: https://www.dof.gob.mx/nota_detalle.php?codigo=4790976&fecha=04/01/1983#gsc.tab=0 (accessed on 28 November 2023).
25. NOM-F-90-S-1978 Determinación de Fibra Cruda en Alimentos. Available online: https://www.dof.gob.mx/nota_detalle.php?codigo=4799842&fecha=27/03/1979#gsc.tab=0 (accessed on 25 November 2023).
26. AOAC Official Method 962.09; Crude Fiber in Animal Feed. AOAC International: Rockville, MD, USA, 2005.
27. Ibitoye, E.B.; Lokman, I.H.; Hezmee, M.N.M.; Goh, Y.M.; Zuki, A.B.Z.; Jimoh, A.A. Extraction and physicochemical characterization of chitin and chitosan isolated from house cricket. *Biomed. Mater.* **2018**, *13*, 025009. [[CrossRef](#)]
28. Nielsen, S.S. *Food Analysis Laboratory Manual*, 3rd ed.; Kluwer Academic/Plenum Publishers: New York, NY, USA, 2003; p. 557.
29. Udomsil, N.; Imsoonthornruksa, S.; Gosalawit, C.; Ketudat-Cairns, M. Nutritional values and functional properties of house cricket (*Acheta domesticus*) and field cricket (*Gryllus bimaculatus*). *Food Sci. Technol. Res.* **2019**, *25*, 597–605. [[CrossRef](#)]
30. Boulos, S.; Tännler, A.; Nyström, L. Nitrogen-to-protein conversion factors for edible insects on the Swiss market: *T. molitor*, *A. domesticus*, and *L. migratoria*. *Front Nutr.* **2020**, *7*, 89. [[CrossRef](#)]
31. AOAC. *Official Methods of Analysis*, 21st ed.; AOAC International: Gaithersburg, MD, USA, 2019.
32. Finke, M.D. Complete nutrient content of four species of feeder insects. *Zoo Biol.* **2013**, *32*, 27–36. [[CrossRef](#)]
33. Bawa, M.; Songsermpong, S.; Kaewtapee, C.; Chanput, W. Effect of diet on the growth performance, feed conversion, and nutrient content of the house cricket. *J. Insect Sci.* **2020**, *20*, 10. [[CrossRef](#)]
34. Psarianos, M.; Ojha, S.; Schneider, R.; Schlüter, O.K. Chitin isolation and chitosan production from house crickets (*Acheta domesticus*) by environmentally friendly methods. *Molecules* **2022**, *27*, 5005. [[CrossRef](#)]

35. Zainol Abidin, N.A.; Kormin, F.; Zainol Abidin, N.A.; Mohamed Anuar, N.A.F.; Abu Bakar, M.F. The potential of insects as alternative sources of chitin: An overview on the chemical method of extraction from various sources. *Int. J. Mol. Sci.* **2020**, *21*, 4978. [[CrossRef](#)]
36. Moreno Villa, F.A. Obtención de Glucosamina Hidroclorada (GlcHCl) a Partir de la Hidrólisis Ácida de Quitina y Quitosano Extraídos de Desecho de Jaiba (*Callinectes arcuatus*). Master's Thesis, Universidad de Sonora, Hermosillo, Sonora, Mexico, 30 June 2010.
37. Lerma, A.G.V. Modificación Estructural de Quitina Mediante Métodos Físicos y Químicos Para su Hidrólisis Enzimática Mediante Quitinasas de *Lecanicillium lecanii*. Doctoral Thesis, Universidad Autónoma Metropolitana, Ciudad de México, Mexico, 23 January 2015.
38. Chen, J.K.; Shen, C.R.; Liu, C.L. N-acetylglucosamine: Production and applications. *Mar. Drugs* **2010**, *8*, 2493–2516. [[CrossRef](#)]
39. Faraldo, M.; Goberna, C. *Técnicas de Análisis y Caracterización de Materiales*, 3rd ed.; Consejo Superior de Investigaciones Científicas: Madrid, Spain, 2021; p. 1052.
40. Pungor, E.; Horvai, G. *A Practical Guide to Instrumental Analysis*, 1st ed.; CRC Press: Boca Raton, FL, USA; London, UK; New York, NY, USA, 2020; p. 288.
41. Dahmane, E.M.; Taourirte, M.; Eladlani, N.; Rhazi, M. Extraction and characterization of chitin and chitosan from *Parapenaeus longirostris* from Moroccan local sources. *Int. J. Polym. Anal. Charact.* **2014**, *19*, 342–351. [[CrossRef](#)]
42. Rehman, K.U.; Hollah, C.; Wiesotzki, K.; Heinz, V.; Aganovic, K.; Rehman, R.U.; Cai, M. Insect-derived chitin and chitosan: A still unexploited resource for the edible insect sector. *Sustainability* **2023**, *15*, 4864. [[CrossRef](#)]
43. Majtán, J.; Bílková, K.; Markovič, O.; Gróf, J.; Kogan, G.; Šimúth, J. Isolation and characterization of chitin from bumblebee (*Bombus terrestris*). *Int. J. Biol. Macromol.* **2007**, *40*, 237–241. [[CrossRef](#)]
44. Sáenz-Mendoza, A.; Zamudio-Flores, P.B.; Palomino-Artalejo, G.A.; Tirado-Gallegos, J.M.; García-Cano, V.G.; Ornelas-Paz, J.J.; Aparicio-Sagüilán, A. Physicochemical, morphological and structural characterization of the chitin and chitosan of *Tenebrio molitor* and *Galleria mellonella* insects. *Rev. Mex. Ing. Quím.* **2019**, *18*, 39–56. [[CrossRef](#)]
45. Martínez, C.M.P. Los fundamentos de la cristalográfica: Una reseña histórica. *An. Quím.* **2014**, *4*, 294–302.
46. Ameh, E.S. A review of basic crystallography and X-ray diffraction applications. *Int. J. Adv. Manuf. Technol.* **2019**, *105*, 3289–3302. [[CrossRef](#)]
47. Mohan, K.; Muralisankar, T.; Jayakumar, R.; Rajeevgandhi, C. A study on structural comparisons of α -chitin extracted from marine crustacean shell waste. *Carbohydr. Polym. Technol.* **2021**, *2*, 100037. [[CrossRef](#)]
48. Kaya, M.; Lelešius, E.; Nagrockaitė, R.; Sargin, I.; Arslan, G.; Mol, A.; Bitim, B. Differentiations of chitin content and surface morphologies of chitins extracted from male and female grasshopper species. *PLoS ONE* **2015**, *10*, e0115531. [[CrossRef](#)]
49. Penagos, J.I.C. Caracterización de materiales a través de medidas de microscopía electrónica de barrido (SEM). *Elementos* **2013**, *3*, 133–146.
50. Rojas, J.; Ciro, Y.; Salamanca, C. Efecto del grado de acetilación en las propiedades farmacocinéticas de quitina extraída de exoesqueletos de camarones. *Vitae* **2018**, *25*, 87.
51. Guinesi, L.S.; Cavalheiro, É.T.G. The use of DSC curves to determine the acetylation degree of chitin/chitosan samples. *Thermochim. Acta* **2006**, *444*, 128–133. [[CrossRef](#)]

Disclaimer/Publisher's Note: The statements, opinions and data contained in all publications are solely those of the individual author(s) and contributor(s) and not of MDPI and/or the editor(s). MDPI and/or the editor(s) disclaim responsibility for any injury to people or property resulting from any ideas, methods, instructions or products referred to in the content.